53rd IEEE Conference on Decision and Control
December 15-17, 2014. Los Angeles, California, USA

A distributed local Kalman consensus filter for traffic estimation

Ye Sun[1] and Daniel B. Work[2]

Abstract— **This work proposes a *distributed local Kalman consensus filter* (DLKCF) for large-scale multi-agent traffic density estimation. The *switching mode model* (SMM) is used to describe the traffic dynamics on a stretch of roadway, and the model dynamics are linear within each mode. The error dynamics of the proposed DLKCF is shown to be *globally asymptotically stable* (GAS) when all freeway sections switch between observable modes. For an unobservable section, we prove that the estimates given by the DLKCF are ultimately bounded. Numerical experiments are provided to show the asymptotic stability of the DLKCF for observable modes, and illustrate the effect of the DLKCF on promoting consensus among various local agents. Supplementary source code is available at https://github.com/yesun/DLKCFcdc2014.**

I. INTRODUCTION

A. Motivation

The unprecedent growth of sensing and computational capacities have advanced the development and implementation of real-time traffic estimation techniques. For a transportation network at the scale of a megacity, a centralized estimator that tracks the entire state of the network requires large and expensive computing resources to meet real-time constraints. An alternative is to partition large networks into local regions, with each region estimated by a cheap commodity computer (e.g. an agent), thus easing the computational burden. However, without coordination between adjacent or overlapping partitions, estimates provided by different agents may disagree on the estimates on the shared boundaries. These motivates the introduction of information sharing among agents to compensate for the lack of a central agent, thus enhancing estimation consistency while also enabling computational scalability.

B. Related Work

A number of sequential state estimation algorithms have been proposed to estimate traffic conditions. The *Switching Mode Model* (SMM) [1]–[3] is a piecewise linear form of the *Cell Transmission Model* (CTM) [4]–[6], and is integrated into the *Mixture Kalman Filter* in [2] for ramp metering. A proof of the stability and a derivation of an error conservation property of a Luenberger observer based on the SMM is provided in [7], which serves as an inspiration for this work and is extended in [8] for more accurate mode estimation. In [9], the *Interacting Multiple Model* algorithm is applied to the SMM with generalized modes. A robust mode selector is proposed in [10] to determine the most probable mode of the uncertain graph-constrained SMM. In [11], a Gaussian approximation of the stochastic traffic model is solved by the standard *Kalman Filter* (KF), and the stochastic observability of the model is proved. The *Parallelized Particle Filters* and the *Parallelized Gaussian Sum Particle Filter* are designed in [12] for computational scalability. Other treatments of traffic estimation include [13]–[17]. A recent overview of sequential estimation techniques for scalar traffic models can be found in [18].

Research on collaborative information processing is driven by the broad applications of multi-agent systems [19]–[22]. The *decentralized Kalman filter* [23], [24] requires a complete communication network with all-to-all links which may not scale in large-scale systems. A scalable *Distributed Kalman Filter* (DKF) is introduced in [25], and [26] partitions the large-scale systems into subsystems to reduce computation load, with observasion fusion applied on the shared states between subsystems to ensure consensus. In the *Kalman-Consensus Filter* (KCF), consensus is achieved by communication on the state estimates [27]. A formal analysis on the stability of the KCF can be found in [27], [28].

C. Contributions and Outline of the Article

The main contribution of this article is the design and analysis of a *Distributed Local Kalman Consensus Filter* (DLKCF) to estimate the traffic density on freeways, with system dynamics chosen to be a piecewise linear form of the *Cell Transmission Model* (CTM) [4]–[6] called the SMM. The transportation network is partitioned into local regions with overlapping areas on the boundaries, and each local region is estimated by an agent. Each agent provides a *local* estimate on its own region, and shares sensor data and state estimates with its *neighbors* (two agents are called neighbors if they communicate with each other). Furthermore, *consensus* on the overlapping areas is pursued to achieve agreement on the estimates of the common state shared between neighbors. We provide a formal proof of the stability and boundedness of the DLKCF, which has been missing from many traffic estimation methods.

This work is organized as follows. Section II summarizes the CTM and the SMM, and Section III introduces the DLKCF. In Section IV-A, we prove that the DLKCF is globally asymptotically stable under the observable modes of the SMM. For the unobservable modes, we prove in Section IV-B that the state estimates are ultimately bounded. Finally, simulation results are presented in Section V.

*This work is supported by a 2012 UIUC CEE Innovation Grant.

[1]Y. Sun is with the Department of Civil and Environmental Engineering and Coordinated Science Laboratory, University of Illinois Urbana-Champaign, Urbana, IL, 61801 USA yesun@illinois.edu

[2]D. Work is an Assistant Professor in the Department of Civil and Environmental Engineering and Coordinated Science Laboratory, University of Illinois Urbana-Champaign, Urbana, IL, 61801 USA dbwork@illinois.edu

II. SCALAR MACROSCOPIC TRAFFIC MODELING

A. Cell Transmission Model

The classical scalar model describing the evolution of traffic density $\rho(t, x)$ on a road network at location x and time t is the *Lighthill-Whitham-Richards* (LWR) *Partial Differential Equation* (PDE) [29], [30], which describes vehicle conservation:

$$\partial_t \rho + \partial_x Q(\rho) = 0. \quad (1)$$

The function $Q(\rho) = \rho v(\rho)$ is called the flux function, where $v(\rho)$ is an empirical velocity function used to close the model. The triangular flux function [5] used in this work is given by

$$Q(\rho) = \begin{cases} \rho v_m & \text{if } \rho \in [0, \rho_c] \\ \rho_c v_m \frac{\rho_m - \rho}{\rho_m - \rho_c} & \text{if } \rho \in [\rho_c, \rho_m], \end{cases} \quad (2)$$

where v_m denotes the *freeflow speed* and ρ_m denotes the *maximum density*. The variable ρ_c is the *critical density* at which the maximum flux is realized. For the triangular fundamental diagram, the flux function has different slopes in *freeflow* ($\rho \le \rho_c$) and *congestion* ($\rho > \rho_c$). In freeflow, the slope is v_m, and in congestion, it is $w = \frac{\rho_c v_m}{\rho_m - \rho_c}$.

The CTM is a discretization of (1) and (2) using a *Godunov scheme* [31]. Consider a discretization grid defined by a space step Δx and a time step Δt. We let l index the cell defined by $x \in [l\Delta x, (l+1)\Delta x)$, and denote ρ_k^l the density at time $k\Delta t$ in cell l. The discretized model (1) becomes

$$\rho_{k+1}^l = \rho_k^l + \frac{\Delta t}{\Delta x}\left(q(\rho_k^{l-1}, \rho_k^l) - q(\rho_k^l, \rho_k^{l+1})\right), \quad (3)$$

where $q(\rho_k^{l-1}, \rho_k^l)$ is the flux between cell $l-1$ and l:

$$q(\rho_k^{l-1}, \rho_k^l) = \min\{v_m \rho_k^{l-1}, w(\rho_m - \rho_k^l), q_m\}, \quad (4)$$

where q_m is the maximum flow given by $q_m = v_m \rho_c$.

B. Switching Mode Model

In the SMM, (3) is written as a hybrid system whose evolution equation switches among different linear modes, depending on the state of the upstream and downstream cells.

1) Definition of modes and evolution equations: Consider discretizing a road section into n cells, and define the state vector of the section to be $\rho_k = \left(\rho_k^1, \cdots, \rho_k^l, \cdots, \rho_k^n\right)^T$. We make the following three assumptions for traffic estimation based on the SMM: (*i*) the densities of the upstream and downstream cells in each section are measured; (*ii*) there is at most one transition between freeflow and congestion within each section; and (*iii*) the boundary density measurements are sufficiently accurate to distinguish between four of the five modes described next, but they cannot determine the location or direction of the shock.

Given the second assumption above, a road section may switch between the following five modes:

1) *freeflow–freeflow* (FF), in which all cells in the section are in freeflow;
2) *congestion–congestion* (CC), in which all cells in the section are in congestion;
3) *congestion–freeflow* (CF), in which the cells in the upstream part of the section are congested, and the cells in the downstream part are in freeflow;
4) *freeflow–congestion 1* (FC1), in which the upstream part of the section is in freeflow, the downstream part is in congestion, and the shock has positive velocity or is stationary; and
5) *freeflow–congestion 2* (FC2), in which the upstream part of the section is in freeflow, the downstream part is in congestion, and the shock has negative velocity.

Note the boundary sensors cannot distinguish between modes 4 and 5. In each mode stated above, the traffic state ρ_k evolves with linear dynamics, forming a hybrid system:

$$\rho_{k+1} = A_{\sigma(k),s(k)}\rho_k + B^\rho_{\sigma(k),s(k)}\boldsymbol{\rho}_m + B^q_{\sigma(k),s(k)}\boldsymbol{q}_m, \quad (5)$$

where $\boldsymbol{\rho}_m = (\rho_m, \cdots, \rho_m)^T \in \mathbb{R}^n$, $\boldsymbol{q}_m = (q_m, \cdots, q_m)^T \in \mathbb{R}^n$, and $A_{\sigma(k),s(k)}$, $B^\rho_{\sigma(k),s(k)}$, $B^q_{\sigma(k),s(k)} \in \mathbb{R}^{n\times n}$ are matrices to be defined precisely later. The mode index $\sigma(k) \in \mathcal{S}$ where $\mathcal{S} = \{1, 2, 3, 4, 5\}$ is the index set denoting the five modes, and $s(k) \in \{0, 1, \cdots, n\}$ is the index introduced to precisely locate the transition between freeflow and congestion when it exists. We say $s(k) = l$ when the transition occurs between cell l and $l+1$.

To explicitly define (5) in each mode, some notation is introduced. For all $p \in \{1, 2, \cdots, n-1\}$, define $\Gamma_p \in \mathbb{R}^{p\times p}$ and $\Delta_p \in \mathbb{R}^{p\times p}$ by their $(i,j)^{\text{th}}$ entries as

$$\Gamma_p(i,j) = \begin{cases} 1 - \frac{v_m \Delta t}{\Delta x} & \text{if } i = j \\ \frac{v_m \Delta t}{\Delta x} & \text{if } i = j+1 \\ 0 & \text{otherwise,} \end{cases}$$

$$\Delta_p(i,j) = \begin{cases} 1 - \frac{w \Delta t}{\Delta x} & \text{if } i = j \\ \frac{w \Delta t}{\Delta x} & \text{if } i = j-1 \\ 0 & \text{otherwise.} \end{cases}$$

In the FF mode, the mode index $\sigma = 1$, and $s(k) = 0$. The explicit forms of $A_{\sigma,s}$, $B^\rho_{\sigma,s}$, and $B^q_{\sigma,s}$ are:

$$A_{1,0} = \begin{pmatrix} 1 & \mathbf{0}_{1,n-1} \\ \begin{pmatrix} \frac{v_m \Delta t}{\Delta x} \\ \mathbf{0}_{n-2,1} \end{pmatrix} & \Gamma_{n-1} \end{pmatrix}, B^\rho_{1,0} = B^q_{1,0} = \mathbf{0}.$$

where $\mathbf{0}_{i,j} \in \mathbb{R}^{i\times j}$ which is zero everywhere, and $\mathbf{0} = \mathbf{0}_{n,n}$.

In the CC mode, the mode index $\sigma = 2$, and $s(k) = n$. The explicit forms of $A_{\sigma,s}$, $B^\rho_{\sigma,s}$, and $B^q_{\sigma,s}$ are:

$$A_{2,n} = \begin{pmatrix} \Delta_{n-1} & \begin{pmatrix} \mathbf{0}_{n-2,1} \\ \frac{w \Delta t}{\Delta x} \end{pmatrix} \\ \mathbf{0}_{1,n-1} & 1 \end{pmatrix}, B^\rho_{2,n} = B^q_{2,n} = \mathbf{0}.$$

In the CF mode, the mode index $\sigma = 3$, and the explicit forms of $A_{\sigma,s}$, $B^\rho_{\sigma,s}$, and $B^q_{\sigma,s}$ are:

$$A_{3,s} = \begin{pmatrix} \Delta_s & \mathbf{0}_{s,n-s} \\ \mathbf{0}_{n-s,s} & \Gamma_{n-s} \end{pmatrix}, B^\rho_{3,s} = \mathbf{0} + \frac{w\Delta t}{\Delta x}E_{s,s},$$

$$B^q_{3,s} = \mathbf{0} - \frac{\Delta t}{\Delta x}E_{s,s+1} + \frac{\Delta t}{\Delta x}E_{s+1,s+1},$$

where $E_{i,j}$ are matrices that are zero everywhere but the $(i,j)^{\text{th}}$ entry, which is one. Note that s may take any value in $\{1,\cdots,n-1\}$, depending on the location of the center of the expansion fan.

In the two FC modes, define $\hat{\Gamma}_p$ and $\hat{\Delta}_p$ as follows:

$$\hat{\Gamma}_p = \begin{cases} \begin{pmatrix} 1 & \mathbf{0}_{1,p} \\ \begin{pmatrix} \frac{v_m \Delta t}{\Delta x} \\ \mathbf{0}_{p-1,1} \end{pmatrix} & \Gamma_p \end{pmatrix} & \text{if } p \in \{1,\cdots,n-1\}, \\ 1 & \text{if } p = 0, \end{cases}$$

and

$$\hat{\Delta}_p = \begin{cases} \begin{pmatrix} \Delta_p & \begin{pmatrix} \mathbf{0}_{1,p-1} \\ \frac{w\Delta t}{\Delta x} \end{pmatrix} \\ \mathbf{0}_{1,p} & 1 \end{pmatrix} & \text{if } p \in \{1,\cdots,n-1\}, \\ 1 & \text{if } p = 0. \end{cases}$$

When $\sigma = 4$ and $s \in \{1,\cdots,n-2\}$, or $\sigma = 5$ and $s \in \{2,\cdots,n-1\}$, the explicit forms of $A_{\sigma,s}$, $B^{\rho}_{\sigma,s}$, and $B^{q}_{\sigma,s}$ are:

$$A_{\sigma,s} = \begin{pmatrix} \hat{\Gamma}_{\tilde{s}-1} & \mathbf{0}_{\tilde{s},1} & \mathbf{0}_{\tilde{s},\bar{s}} \\ \begin{pmatrix} \mathbf{0}_{1,\tilde{s}-1} & \frac{v_m\Delta t}{\Delta x} \end{pmatrix} & 1 & \begin{pmatrix} \frac{w\Delta t}{\Delta x} & \mathbf{0}_{1,\bar{s}-1} \end{pmatrix} \\ \mathbf{0}_{\bar{s},\tilde{s}} & \mathbf{0}_{\bar{s},1} & \hat{\Delta}_{\bar{s}-1} \end{pmatrix},$$

$$B^{\rho}_{\sigma,s} = \begin{pmatrix} \mathbf{0}_{\tilde{s}+1,\tilde{s}+1} & \begin{pmatrix} \mathbf{0}_{\tilde{s},1} & \mathbf{0}_{\tilde{s},\bar{s}-1} \\ -\frac{w\Delta t}{\Delta x} & \mathbf{0}_{1,\bar{s}-1} \end{pmatrix} \\ \mathbf{0}_{\bar{s},\tilde{s}+1} & \mathbf{0}_{\bar{s},\bar{s}} \end{pmatrix}, B^{q}_{\sigma,s} = \mathbf{0},$$

where for $\sigma = 4$ we have $\tilde{s} = s$ and $\bar{s} = n-s-1$, and for $\sigma = 5$ we have $\tilde{s} = s-1$ and $\bar{s} = n-s$.

When $\sigma = 4$ and $s = n-1$, we have $A_{\sigma,s} = \text{diag}\left(\hat{\Gamma}_{n-2}, 1\right)$ (i.e. with $\hat{\Gamma}_{n-2}$ and 1 on the diagonal) , and $A_{\sigma,s} = \text{diag}\left(1, \hat{\Delta}_{n-2}\right)$ when $\sigma = 5$ and $s = 1$. For both cases, we have $B^{\rho}_{\sigma,s} = B^{q}_{\sigma,s} = \mathbf{0}$.

2) Observability: The observability results of the SMM for individual modes are summarized in Table I [3]. It can be derived directly from standard linear system techniques for each mode given (5) and the observation equation:

$$z_k = H_k \rho_k, \tag{6}$$

where z_k is the measurement vector, and H_k is the output matrix.

Remark 1. *In the SMM proposed in [1]–[3], an additional assumption requires the precise inflow and outflow of the section as inputs of the system. Here we instead assign constant dynamics for the boundary cells subject to some uncertainty. It is assumed that boundary measurements will be available and will be integrated through the update equation within the filter. As a result the system dynamics no longer depends on cell densities outside the section, at the expense of a correct model at the boundary. This treatment is made since: (i) measurements of boundary conditions cannot be treated as the true input of the system without accounting for measurement errors, and (ii) for distributed computational platforms, independence of system dynamics for each section is desirable. Note that all results and proofs in this article hold for either formulation.*

TABLE I

OBSERVABILITY OF THE SMM[1,2] [3]

Mode	U	D	Shock velocity	Observable with
1	F	F	No shock	D measurement
2	C	C	No shock	U measurement
3	C	F	No shock	U and D measurements
4	F	C	positive or stationary	unobservable
5	F	C	negative	unobservable

[1] F and C represent freeflow and congested, respectively.
[2] U and D represent upstream and downstream, respectively.

III. DISTRIBUTED LOCAL KALMAN CONSENSUS FILTERING

A. Kalman Filter

In this section, we briefly review the KF and introduce notation needed later in the proposed filter. Consider a linear time-varying model

$$\rho_{k+1} = A_k \rho_k + w_k,\ \rho_k \in \mathbb{R}^n, \tag{7}$$

where $w_k \sim \mathcal{N}(0, Q_k)$. Sensor measurements z_k are modeled by the following linear observation equation

$$z_k = H_k \rho_k + v_k,\ z_k \in \mathbb{R}^m, \tag{8}$$

where H_k and $v_k \sim \mathcal{N}(0, R_k)$ are the observation matrix and measurement noise, respectively.

Given the sensor data up to time k denoted by $Z_k = \{z_0,\cdots,z_k\}$, the *prior estimate* and *posterior estimate* of the state can be expressed as $\rho_{k|k-1} = E[\rho_k|Z_{k-1}]$ and $\rho_{k|k} = E[\rho_k|Z_k]$, respectively. Let $\eta_{k|k-1} = \rho_{k|k-1} - \rho_k$ and $\eta_{k|k} = \rho_{k|k} - \rho_k$ denote the prior and posterior estimation errors. The state error covariance matrices associated with $\rho_{k|k-1}$ and $\rho_{k|k}$ are given by $\Gamma_{k|k-1} = E[\eta_{k|k-1}\eta^T_{k|k-1}]$ and $\Gamma_{k|k} = E[\eta_{k|k}\eta^T_{k|k}]$. The KF sequentially computes $\rho_{k|k}$ from $\rho_{k-1|k-1}$ as follows:

$$\text{Forecast:} \begin{cases} \rho_{k|k-1} = A_{k-1}\rho_{k-1|k-1} \\ \Gamma_{k|k-1} = A_{k-1}\Gamma_{k-1|k-1}A^T_{k-1} + Q_{k-1}, \end{cases}$$

$$\text{Analysis:} \begin{cases} \rho_{k|k} = \rho_{k|k-1} + K_k(z_k - H_k\rho_{k|k-1}) \\ \Gamma_{k|k} = \Gamma_{k|k-1} - K_k H_k \Gamma_{k|k-1} \\ K_k = \Gamma_{k|k-1}H^T_k(R_k + H_k\Gamma_{k|k-1}H^T_k)^{-1}. \end{cases}$$

B. Distributed Local Kalman Consensus Filter

The DLKCF is a localized version of the KCF, which itself is an extension of the KF for multi-agent estimation [27], [28]. Consider a network with an ad hoc undirected communication topology between agents given by the graph $\mathcal{G} = (\mathcal{V}, \mathcal{E})$, where $\mathcal{V}$ and $\mathcal{E}$ are the vertex and edge sets, respectively. For agent i the output equation is given by

$$z^{\text{d}}_{i,k} = H^{\text{d}}_{i,k}\rho_k + v^{\text{d}}_{i,k},\ z^{\text{d}}_{i,k} \in \mathbb{R}^{m_i},$$

where the superscript d stands for distributed, and $v^{\text{d}}_{i,k} \sim \mathcal{N}\left(0, R^{\text{d}}_{i,k}\right)$. Let $\mathcal{N}_i = \{j : (i,j) \in \mathcal{E}\}$ be the set of neighboring agents of agent i on graph $\mathcal{G}$, and define $\mathcal{J}_i = \mathcal{N}_i \bigcup \{i\}$. In the KCF, through communication each agent possesses columnized measurement vector $z_{i,k} =$

$\text{col}_{j\in\mathcal{J}_i}\left(z^{\text{d}}_{j,k}\right)$ and a corresponding columnized output matrix $H_{i,k} = \text{col}_{j\in\mathcal{J}_i}\left(H^{\text{d}}_{j,k}\right)$, as well as a block diagonal measurement error covariance matrix $R_{i,k} = \text{diag}_{j\in\mathcal{J}_i}\left(R^{\text{d}}_{j,k}\right)$. A consensus term is computed based on the disparities of the prior estimates among neighbors and is applied to the analysis step to promote agreement on estimates among neighboring agents.

For the KCF stated above, each agent estimates all the state variables of ρ_k. However, for estimation on large-scale transportation systems, this is neither computationally efficient nor practically necessary. Consequently, a localized version of the KCF, namely the DLKCF, is introduced. The DLKCF partitions the state into local overlapping subsets, and each agent estimates a single subset of the state.

The freeway network is partitioned into N local sections, with overlapping regions established to allow communication between neighboring agents to exchange messages on measurements and state estimates. From the SMM in section II-B, the system dynamics of the i^{th} section is given by

$$\rho_{i,k+1} = A_{i,k}\rho_k + B^{\rho}_{i,k}\boldsymbol{\rho}_m + B^{q}_{i,k}\boldsymbol{q}_m, \rho_{i,k} \in \mathbb{R}^{n_i}. \tag{9}$$

Note that in (9) and for the remainder of the article the subscripts for A, B^ρ, and B^q are slightly different from what was used in (5) with $\sigma(k)$ and $s(k)$. Since both $\sigma(k)$ and $s(k)$ are dependent on k, we let subscript k combine their effects, and add an subscript $i \in \mathcal{I} = \{1, 2, \cdots, N\}$ to denote the section index. We denote the dimension of the overlapping region between section i and section j as $n_{i,j}$. For the freeway network, the neighborhood of section i is defined as

$$\mathcal{N}_i = \begin{cases} \{i+1\} & \text{if } i = 1 \\ \{i-1, i+1\} & \text{if } i \neq 1, \text{ and } i \neq N \\ \{i-1\} & \text{if } i = N. \end{cases}$$

For $j \in \mathcal{N}_i$, define matrix operator $\hat{I}_{i,j}$ as

$$\hat{I}_{i,j} = \begin{cases} \begin{pmatrix} I_{n_{i,j}} & \mathbf{0}_{n_{i,j}, n_i - n_{i,j}} \end{pmatrix} & \text{if } j = i-1 \\ \begin{pmatrix} \mathbf{0}_{n_{i,j}, n_i - n_{i,j}} & I_{n_{i,j}} \end{pmatrix} & \text{if } j = i+1, \end{cases} \tag{10}$$

where $I_{n_{i,j}} \in \mathbb{R}^{n_{i,j}}$ is the identity matrix, and the operation $\hat{I}_{i,j}\rho_{i,k}$ selects the part of agent i's state that overlaps with agent j.

Formally the forecast and analysis steps of the DLKCF for the i^{th} agent are written as

$$\begin{cases} \rho_{i,k|k-1} = A_{i,k-1}\rho_{i,k-1|k-1} \\ \Gamma_{i,k|k-1} = A_{i,k-1}\Gamma_{i,k-1|k-1}A^T_{i,k-1} + Q_{i,k-1}, \end{cases} \tag{11}$$

$$\begin{cases} \rho_{i,k|k} &= \rho_{i,k|k-1} + K_{i,k}\left(z_{i,k} - H_{i,k}\rho_{i,k|k-1}\right) \\ & \quad + \sum_{j\in\mathcal{N}_i} C^j_{i,k}\left(\hat{I}_{j,i}\rho_{j,k|k-1} - \hat{I}_{i,j}\rho_{i,k|k-1}\right) \\ \Gamma_{i,k|k} &= \Gamma_{i,k|k-1} - K_{i,k}H_{i,k}\Gamma_{i,k|k-1} \\ K_{i,k} &= \Gamma_{i,k|k-1}H^T_{i,k}(R_{i,k} + H_{i,k}\Gamma_{i,k|k-1}H^T_{i,k})^{-1}, \end{cases} \tag{12}$$

where $C^j_{i,k}$ is the *consensus gain* of agent i associated with neighbor j at time step k, and for simplicity we drop the last two terms in (9) independent of the state. Our choice for the consensus gain for the observable modes is inspired by [28], and the consensus term is dropped for the unobservable modes. Hence the choice of the consensus gain reads:

$$C^j_{i,k} = \begin{cases} \gamma_{k-1}F_{i,k}G_{i,k}\hat{I}^T_{i,j} & \sigma(k) \in \{1,2,3\} \\ \mathbf{0} & \sigma(k) \in \{4,5\}, \end{cases} \tag{13}$$

where

$$\begin{aligned} F_{i,k} =& I - K_{i,k}H_{i,k}, \\ G_{i,k} =& A_{i,k-1}\Gamma_{i,k-1|k-1}A^T_{i,k-1} + Q_{i,k-1} \\ &+ \Gamma_{i,k|k-1}S_{i,k}\Gamma_{i,k|k-1}, \end{aligned} \tag{14}$$

where $S_{i,k} = H^T_{i,k}R^{-1}_{i,k}H_{i,k}$ is the *information matrix*, and γ_k is a sufficiently small scaling factor, whose explicit form will be given in Section IV to ensure stability of the filter.

IV. STABILITY AND PERFORMANCE ANALYSIS OF THE DLKCF FOR TRAFFIC ESTIMATION

In this section, we show that for a network where all sections switch among observable modes, the error dynamics is *globally asymptotically stable* (GAS). For an unobservable section, we show that despite the lack of knowledge on the state equations and boundary conditions, the estimate of the state is physically meaningful.

A. Asymptotic Stability of Error Dynamics in Observable Modes

We define the prior and posterior estimation errors for section i as $\eta_{i,k|k-1} = \rho_{i,k|k-1} - \rho_{i,k}$ and $\eta_{i,k|k} = \rho_{i,k|k} - \rho_{i,k}$, and define the neighbor disagreement as

$$u^j_{i,k} = \hat{I}_{j,i}\eta_{j,k|k-1} - \hat{I}_{i,j}\eta_{i,k|k-1}. \tag{15}$$

The global estimation error $\eta_{k|k}$ is reconstructed by $\eta_{k|k} = \text{col}(\eta_{1,k|k}, \cdots, \eta_{N,k|k})$, and the estimation error in section i evolves as follows (without model and measurement noise):

$$\eta_{i,k|k} = F_{i,k}A_{i,k-1}\eta_{i,k-1|k-1} + \sum_{j\in\mathcal{N}_i} C^j_{i,k}u^j_{i,k}. \tag{16}$$

We choose a *common Lyapunov function* which reads

$$V(k, \eta_{k|k}) = \sum_{i=1}^{N} \eta^T_{i,k|k}\Gamma^{-1}_{i,k|k}\eta_{i,k|k}, \tag{17}$$

and compute its one-step change $\delta V(k, \eta_{k|k})$ by applying (16) as follows:

$$\begin{aligned} &\delta V(k, \eta_{k|k}) = V(k+1, \eta_{k+1|k+1}) - V(k, \eta_{k|k}) = \\ &\textstyle\sum_{i=1}^N \eta^T_{i,k|k}\left(A^T_{i,k}F^T_{i,k+1}\Gamma^{-1}_{i,k+1|k+1}F_{i,k+1}A_{i,k} - \Gamma^{-1}_{i,k|k}\right) \times \\ &\eta_{i,k|k} \\ &+2\textstyle\sum_{i=1}^N\left(\eta^T_{i,k+1|k}F^T_{i,k+1}\Gamma^{-1}_{i,k+1|k+1}\sum_{j\in\mathcal{N}_i} C^j_{i,k+1}u^j_{i,k+1}\right) \\ &+\textstyle\sum_{i=1}^N\left(\sum_{j\in\mathcal{N}_i} C^j_{i,k+1}u^j_{i,k+1}\right)^T\Gamma^{-1}_{i,k+1|k+1}\times \\ &\left(\textstyle\sum_{j\in\mathcal{N}_i} C^j_{i,k+1}u^j_{i,k+1}\right). \end{aligned} \tag{18}$$

The common Lyapunov function (17) is *radically unbounded* by the following lemma.

Lemma 1 (Boundedness of the estimation error covariance matrix in the KF for an arbitrary switching sequence in observable modes [32]). *If the hybrid system* (9) *switches among observable modes for all i and k, the error covariance matrix $\Gamma_{i,k|k}$ given in* (12) *is bounded for all i and k, independent of the switching sequence.*

The next lemma provides a result on the Laplacian of an undirected graph, which is important for treatment of the consensus term in the stability proof of the DLKCF.

Lemma 2 (Quadratic property of the Laplacian of an undirected graph [33], [34])**.** *The following holds for the n-dimensional Laplacian $\bar{L}$ of any undirected graph $\mathcal{G} = (\mathcal{V}, \mathcal{E})$ with N vertices, irrespective of its connectivity:*

$$\sum_{i=1}^{N}\sum_{j\in\mathcal{N}_i}\xi_i(\xi_j-\xi_i) = -\frac{1}{2}\sum_{(i,j)\in\mathcal{E}}\|\xi_j-\xi_i\|^2 = -\xi^T\bar{L}\xi,$$

where $\xi = col(\xi_1, \cdots, \xi_N)$ with $\xi_i \in \mathbb{R}^n$ the element corresponding to the i^{th} vertex of $\mathcal{V}$, and $\bar{L} = I_n \otimes L$ with L the graph Laplacian of $\mathcal{G}$.

The GAS result for the DLKCF in observable modes is presented next.

Proposition 1 (Stability of the DLKCF for observable modes)**.** *Consider the DLKCF in* (11) *and* (12) *with the consensus gain in* (13)–(14)*. Suppose $Q_{i,k}$ is positive definite for all i and k, and all sections switch among the observable modes of the SMM. Then, the error dynamics of $\eta_{k|k}$ is GAS for sufficiently small γ_k, with consensus reached on the overlapping regions between neighbors.*

Proof. We show $\delta V(k, \eta_{k|k})$ is negative when $\eta_{k|k} \neq 0$. To determine the sign of $\delta V(k, \eta_{k|k})$, we first analyse the signs of the three terms in (18) independently and then combine them together.

Step 1. Negative definiteness of the first term in δV

The proof for the first term follows closely from [28] with minor changes. Here we only show the result and introduce the matrices needed in this article. Each element in the first term in δV can be equivalently written as

$$\begin{aligned}&\eta_{i,k|k}^T\left(A_{i,k}^TF_{i,k+1}^T\Gamma_{i,k+1|k+1}^{-1}F_{i,k+1}A_{i,k}-\Gamma_{i,k|k}^{-1}\right)\eta_{i,k|k}\\ =&-\eta_{i,k|k}^T\Lambda_{i,k}\eta_{i,k|k} = -\eta_{k|k}^T\Lambda_k\eta_{k|k},\end{aligned}$$

where $\Lambda_k = \mathrm{diag}(\Lambda_{1,k}, \cdots, \Lambda_{n,k})$. It can be shown that

$$\begin{aligned}\Lambda_{i,k} =&\Gamma_{i,k|k}^{-1} - A_{i,k}^T(A_{i,k}\Gamma_{i,k|k}A_{i,k}^T + W_k)^{-1}A_{i,k} > 0,\\ W_k =&Q_{i,k} + \Gamma_{i,k+1|k}S_i\Gamma_{i,k+1|k} > 0,\end{aligned}$$

by assuming $Q_{i,k} > 0$. Consequently, the first term is negative definite.

Step 2. Negative semidefiniteness of the second term in δV

Using the quadratic property of the Laplacian in Lemma 2, we can render the second term of δV negative semidefinite by the consensus gain chosen in (13)–(14). We introduce a new undirected graph $\hat{\mathcal{G}} = (\hat{\mathcal{V}}, \hat{\mathcal{E}})$ representing the topology of the overlapping regions with $\hat{\mathcal{V}}_k = \{\hat{\xi}_{\hat{i},k} : \hat{i} \in \hat{\mathcal{I}}\}$ for $\hat{\mathcal{I}} = \{1, \cdots, 2N-2\}$, and

$$\hat{\xi}_{\hat{i},k} = \begin{cases}\hat{I}_{i,j}\eta_{i,k|k-1} & \text{with } i=\frac{\hat{i}+1}{2},\ j=i+1, \text{ if } \hat{i} \text{ odd}\\ \hat{I}_{j,i}\eta_{j,k|k-1} & \text{with } i=\frac{\hat{i}}{2},\ j=i+1, \text{ if } \hat{i} \text{ even,}\end{cases}$$

$$\mathcal{N}_{\hat{i}} = \begin{cases}\{\hat{i}+1\} & \text{if } \hat{i} \text{ odd}\\ \{\hat{i}-1\} & \text{if } \hat{i} \text{ even.}\end{cases}$$

Suppose $n_{i,j} = \hat{n}$ for all $i \in \mathcal{I}$ and for all $j \in \mathcal{N}_i$, then $\hat{\xi}_{\hat{i},k} \in \mathbb{R}^{\hat{n}}$ for all $\hat{i}$. Let $\hat{L}$ be the $\hat{n}$ dimensional Laplacian of $\hat{\mathcal{G}}$. Denote $\hat{\xi}_k = \mathrm{col}(\hat{\xi}_{1,k}, \cdots, \hat{\xi}_{2N-2,k}) = \hat{H}\eta_{k|k-1}$, where $\hat{H} = \mathrm{Diag}(\hat{H}_1, \cdots, \hat{H}_n)$ with the i^{th} block on the diagonal

$$\hat{H}_i = \begin{cases}\hat{I}_{i,i+1} & \text{if } i=1\\ \hat{I}_{i,i-1} & \text{if } i=n\\ \left(\hat{I}_{i,i-1}^T\ \hat{I}_{i,i+1}^T\right)^T & \text{otherwise,}\end{cases}$$

and let $A_k = \mathrm{diag}(A_{1,k}, \cdots, A_{N,k})$. Then by substituting the consensus gain (13) and the neighbor disagreement (15) into the second term of δV, and rewriting it in terms of the new graph $\hat{\mathcal{G}}$, we obtain:

$$\begin{aligned}&2\sum_{i=1}^{N}\left(\eta_{i,k+1|k}^TF_{i,k+1}^T\Gamma_{i,k+1|k+1}^{-1}\sum_{j\in\mathcal{N}_i}C_{i,k+1}^ju_{i,k+1}^j\right)\\ =&-2\gamma_k\eta_{k|k}^TA_k^T\hat{H}^T\hat{L}\hat{H}A_k\eta_{k|k} \leq 0.\end{aligned}$$

Thus it is concluded that the second term in δV is negative semidefinite.

Step 3. Positive definiteness of the third term in δV

Given the choice of consensus gain in (13)–(14), the third term in δV can be written as

$$\begin{aligned}&\sum_{i=1}^{N}\left(\sum_{j\in\mathcal{N}_i}C_{i,k+1}^ju_{i,k+1}^j\right)^T\Gamma_{i,k+1|k+1}^{-1}\left(\sum_{j\in\mathcal{N}_i}C_{i,k+1}^ju_{i,k+1}^j\right)\\ &=\gamma_k^2\sum_{i=1}^{N}\left(\sum_{j\in\mathcal{N}_i}\hat{I}_{i,j}^Tu_{i,k+1}^j\right)^TG_{i,k+1}^T\left(\sum_{j\in\mathcal{N}_i}\hat{I}_{i,j}^Tu_{i,k+1}^j\right).\end{aligned}$$

We columnize $u_{i,k}^j$ over all neighbors $j \in \mathcal{N}_i$ within each section i and over all sections $i \in \mathcal{I}$, and denote it as u_k:

$$u_k = \mathrm{col}_{i\in\mathcal{I}}\left(\mathrm{col}_{j\in\mathcal{N}_i}\left(u_{i,k}^j\right)\right) = \tilde{L}\eta_{k|k-1} = \tilde{L}A_{k-1}\eta_{k-1|k-1},$$

where $\tilde{L}$ can be defined as a partitioned matrix with the $(\hat{i}, i)^{\text{th}}$ block $\tilde{L}_{\hat{i},i}$ given by

$$\tilde{L}_{\hat{i},i} = \begin{cases}-\hat{I}_{i,i+1} & \text{if } \hat{i} \text{ is odd, and } i=\frac{1}{2}(\hat{i}+1)\\ \hat{I}_{i,i-1} & \text{if } \hat{i} \text{ is odd, and } i=\frac{1}{2}(\hat{i}+1)+1\\ \hat{I}_{i,i+1} & \text{if } \hat{i} \text{ is even, and } i=\frac{\hat{i}}{2}\\ -\hat{I}_{i,i-1} & \text{if } \hat{i} \text{ is even, and } i=\frac{\hat{i}}{2}+1\\ \mathbf{0} & \text{otherwise,}\end{cases}$$

where $\hat{i} \in \hat{\mathcal{I}}$ and $i \in \mathcal{I}$. Denoting $G_k = \mathrm{diag}(G_{1,k}, \cdots, G_{N,k})$, the third term in δV is equivalent to

$$\begin{aligned}&\gamma_k^2\sum_{i=1}^{N}\left(\sum_{j\in\mathcal{N}_i}\hat{I}_{i,j}^Tu_{i,k+1}^j\right)^TG_{i,k+1}^T\left(\sum_{j\in\mathcal{N}_i}\hat{I}_{i,j}^Tu_{i,k+1}^j\right)\\ =&\gamma_k^2\eta_{k|k}^TA_k^T\tilde{L}^T\hat{H}G_{k+1}\hat{H}^T\tilde{L}A_k\eta_{k|k} > 0,\end{aligned}$$

and it is positive definite since G_{k+1} is positive definite.

Step 4. The negative definiteness of $\delta V(k,\eta_{k|k})$

Provided Steps 1, 2, and 3, δV can be written as

$$\delta V(k,\eta_{k|k}) = -\eta_{k|k}^T\left(\Lambda_k - \gamma_k^2 A_k^T \tilde{L}^T \hat{H} G_{k+1} \hat{H}^T \tilde{L} A_k\right)\eta_{k|k} - 2\gamma_k \eta_{k|k}^T A_k^T \hat{H}^T \tilde{L} \hat{H} A_k \eta_{k|k}.$$

Therefore by choosing γ_k sufficiently small we can render $\delta V(k,\eta_{k|k}) < 0$ for all $k \geq 0$ and for all $\eta_{k|k} \neq 0$. To be more precise, we need $\gamma_k < \gamma_k^*$ where γ_k^* is defined by

$$\gamma_k^* = \left(\frac{\lambda_{\min}(\Lambda_k)}{\lambda_{\max}\left(A_k^T \tilde{L}^T \hat{H} G_{k+1} \hat{H}^T \tilde{L} A_k\right)}\right)^{\frac{1}{2}},$$

where $\lambda_{\min}$ and $\lambda_{\max}$ are the minimum and maximum eigenvalues of a matrix, respectively. Thus we conclude that $\delta V(k,\eta_{k|k}) < 0$ for all $k \geq 0$ and for all $\eta_{k|k} \neq 0$, and therefore $\eta_{k|k} = 0$ is GAS for the error dynamics of the DLKCF. Consequently, all estimators reach a consensus on the overlapping regions between neighbors. □

B. Ultimate Boundedness of Estimates in Unobservable Modes

Challenges for estimating the unobservable sections stem from the dependence of the system dynamics of the SMM on the state to be estimated (i.e. mode, shock location and shock velocity), thus non-observability of the system will lead to unknown system dynamics. Moreover, with only upstream and downstream measurements, it can be shown that the unobservable modes are also undetectable. In this section we show that the estimates of all the cells in an unobservable section are ultimately bounded inside $[-\varepsilon, \rho_m+\varepsilon]$ for all $\varepsilon > 0$, provided that the upstream and downstream measurements are available. This property ensures that the estimates given by the DLKCF for unobservable modes are always physically meaningful to within ε.

First we present a lemma stating the boundedness of Kalman gain K_k, which is necessary for the boundedness of the estimates.

Lemma 3 (Boundedness of the Kalman gain for an undetectable system [35])**.** *If the system* (7)-(8) *is undetectable, and all the undetectable modes are of unit modulus, then K_k is uniformly bounded from above for all $k \geq 0$.*

The *Kalman observability canonical form* of (5)-(6) shows that the eigenvalues of the observable subspace (i.e. the boundary cells) are one, and the unobservable subsystem has eigenvalues less than or equal to one (with the eigenvalue one corresponding to the shock location), which satisfies the assumptions of Lemma 3. We now establish the ultimate boundedness of the estimates, and for the remainder of Section IV-B the section index i is dropped for notational simplicity.

Proposition 2 (Ultimate boundedness of the DLKCF for an unobservable section)**.** *Consider an unobservable section in a road network with dimension n. For all $\varepsilon > 0$, a finite time $T(\varepsilon)$ exists such that $\rho_{k|k}^l \in [-\varepsilon, \rho_m + \varepsilon]$ for all $k > T(\varepsilon)$ and for all $l \in \{1,\cdots,n\}$, independent of the initial estimate.*

Proof. The proof is by induction. For all $\varepsilon > 0$, since the upstream cell is in the observable subspace, we have $\rho_{k|k}^1 \to \rho_k^1$, where $\rho_k^1 \geq 0$. Hence a finite time $T_1(\varepsilon)$ exists such that $\rho_{k|k}^1 > -\frac{\varepsilon}{n}$ for all $k > T_1(\varepsilon)$.

Suppose $\rho_{k|k}^{l-1} > -\frac{(l-1)\varepsilon}{n}$. For all $l \in \{2,\cdots,n\}$, if $\rho_{k|k}^l < -\frac{(l-1)\varepsilon}{n}$, we obtain from (4) that

$$q\left(\rho_{k|k}^{l-1},\rho_{k|k}^l\right) = v_m \rho_{k|k}^{l-1} > -v_m\frac{(l-1)\varepsilon}{n}, \quad (19)$$

$$q\left(\rho_{k|k}^{l},\rho_{k|k}^{l+1}\right) \leq v_m \rho_{k|k}^{l}. \quad (20)$$

Combining (19) and (20) with (3), and adding an information update term from the analysis step yields

$$\rho_{k+1|k+1}^l > \rho_{k|k}^l + \frac{v_m \Delta t}{\Delta x}\left|\rho_{k|k}^l + \frac{(l-1)\varepsilon}{n}\right| - c \parallel \eta_{k|k}^o \parallel_\infty,$$

where $c > 0$ is a finite scalar whose existence is guaranteed by the boundedness of Kalman gain, and we denote $\eta_{k|k}^o = \left(\eta_{k|k}^1, \eta_{k|k}^n\right)^T$ as the posterior estimation error of the upstream and downstream cells, which form an observable subspace, hence $\parallel \eta_{k|k}^o \parallel_\infty \to 0$ as $k \to \infty$. Thus a class $\mathcal{K}$ function $\alpha(\cdot)$ and a continuous positive definite function $\mathcal{W}(|\cdot|)$ on $\mathbb{R}$ exist such that

$$\rho_{k+1|k+1}^l - \rho_{k|k}^l > \mathcal{W}\left(\left|\rho_{k|k}^l + \frac{(l-1)\varepsilon}{n}\right|\right),$$

$$\forall \left|\rho_{k|k}^l + \frac{(l-1)\varepsilon}{n}\right| \geq \alpha\left(\parallel \eta_{k|k}^o \parallel_\infty\right),$$

which indicates that the one-step change of the estimates is always positive, and large enough so that a finite time $T_l(\varepsilon)$ exists such that $\rho_{k|k}^l > -\frac{l\varepsilon}{n}$ for all $k > T_l(\varepsilon)$ [36]. By induction we conclude that if $\rho_{k|k}^{n-1} > -\frac{(n-1)\varepsilon}{n}$, a finite time $T_n(\varepsilon)$ exists such that $\rho_{k|k}^n > -\varepsilon$ for all $k > T_n(\varepsilon)$. Letting $T(\varepsilon) = \max_l\{T_l(\varepsilon)\} = T_n(\varepsilon)$, we obtain $\rho_{k|k}^l > -\varepsilon$ for all $k > T(\varepsilon)$ and $l \in \{1,2,\cdots,n\}$. This proves the ultimate lower bound of the estimates.

The proof for an ultimate upper bound is similar, with a variation that the induction is conducted from n to 1. □

The essence of ultimate boundedness is that it rules out the possibility that the estimate of any single cell in the unobservable section is destabilized by the analysis step, thus it is not necessary to drop the output feedback as in [7] for the Luenberger observer. In future work we will show that under most cases the error sum over the cells in the unobservable section is converging.

V. NUMERICAL EXPERIMENTS

In this section, we assess the performance of the DLKCF under different scenarios. We first show the estimation results of the DLKCF for a *Riemann problem* [37], and validate the GAS of error dynamics under observable modes when

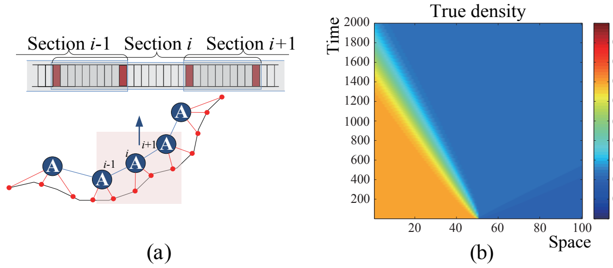

Fig. 1. a) Freeway network setup and the communication topology between estimation agents (capital A in circles) and sensors (red dots), with blue lines standing for connections between agents, and red lines representing connections between agent and sensors. The network is simplified into a one-dimensional straight line, discretized by cells (small rectangles) and localized by sections (blocks). Sensor locations are represented by shaded cells; b) True solution of a Riemann problem (expansion fan).

properly accounting for the modeling errors on the boundaries. Then under a more complex experiment, we evaluate the performance of the consensus filter by comparing the disagreements on estimates among neighbors with and without a consensus term. The computation complexity of the DLKCF at each step is dominated by $O\left(n_i^3 + n_i^2 \hat{n}\right)$ for the i^{th} agent[1], which is much smaller than $O\left(n^3\right)$, the cost for a centralized KF, when $n_i \ll n$.

A. GAS under Observable Modes

We first present an experiment where the initial condition of the entire network is piecewise constant, and the true solution is approximated using the Godunov scheme (3). We show that the negative effect of assigning constant boundary dynamics in our SMM can be attenuated by imposing larger modeling errors on the corresponding boundaries.

The network setup and the communication topology is illustrated in Fig. 1a. The network is a stretch of highway divided into 100 cells and 5 sections. For the DLKCF, each section has 28 cells, with the left and right 10 cells overlapping with its left and right neighbors, respectively.

We apply normalized parameters for the triangular fundamental diagram, and analyse the behaviour of the DLKCF when the true solution is an expansion fan (shown in Fig. 1b). Parameter values which are not detailed here can be found in the supplementary source code.

The estimation of the expansion fan given by the DLKCF is illustrated in Fig. 2a. Note that in order to validate the GAS of estimation error, measurement noise is turned off for this experiment to check the convergence of the estimation error (in mean) to zero. The evolution of the common Lyapunov function (17) is plotted in Fig. 2b, with the solid line denoting the common Lyapunov function for the estimate in Fig. 2a, and with the dashed line denoting an estimate when the standard deviation of model noise is increased to 0.3 at the boundary cells with constant dynamics (compared to 0.03 at the interior cells). It is shown that by increasing the standard deviation of model noise on the boundary we yield a monotonically decreasing common Lyapunov function.

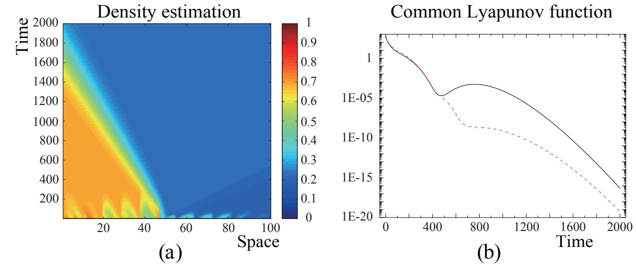

Fig. 2. Estimation of an expansion fan. a) State estimates by the DLKCF; b) Evolution of the common Lyapunov function without (solid line) and with (dashed line) increases on the standard deviations of model noise on the boundary cells.

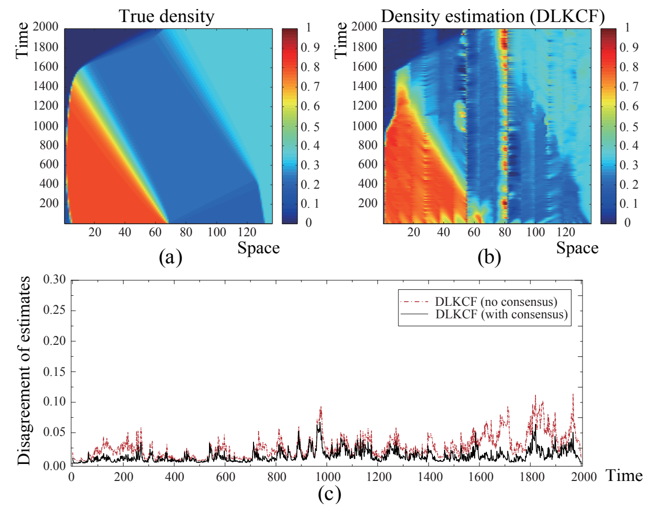

Fig. 3. a) True solution defined as a combination of an expansion fan and a shock propagating upstream, with a sinusoidal boundary condition; b) State estimation by the DLKCF; c) Disagreement on estimates u_k for the DLKCF with and without the consensus term.

B. Effect of the Consensus Filter

In this section, we show the effect of the DLKCF on reducing the disagreement of estimates on the overlapping cells given by adjacent agents. We compare the performances of the DLKCF with and without a consensus term. The true solution is set to be a combination of an expansion fan and a shock propagating upstream, with a sinusoidal upstream boundary condition (illustrated in Fig. 3a.)

Disagreement between estimates provided by different agents can stem from various aspects. For this experiment we generate disagreement by imposing the combining effect of the low quality sensors, the low quality agents, and disagreement on model parameters used by different agents in estimation. Starting from the downstream sensor of the first section, we put a low-quality sensor with a large measurement error once every three sensors, and we assume that agents indexed by even numbers cannot recognize the low-quality sensors they are connected to. We also apply different values of ρ_m, ρ_c, and v_m in the estimator for agents

[1]It is assumed that the *Rayleigh Quotient Iteration* is applied for rapid convergence when computing eigenvalues in the consensus term. Also note that the sparsity of the matrices A_k, $\tilde{L}$ and $\hat{H}$ is not considered currently.

indexed by odd and even numbers. The disagreement at time k is computed by $u_k = \frac{1}{N-1}\sum_{i=1}^{N-1}\frac{\|u_{i,k}^{i+1}\|_2^2}{n_{i,i+1}}$ with $u_{i,k}^{i+1}$ defined in (15). Fig. 3b shows the estimation given by the DLKCF, where the large estimation errors at regions around cell 80 are generated because the corresponding section is processing low-quality sensor data whose large errors are not recognized. Fig. 3c compares the disagreements δ_k of the DLKCF with and without a consensus term. It is shown that the disagreement can always be reduced by the consensus term in the DLKCF. Moreover, in general the effect of the consensus term is more apparent if the disagreement before applying a consensus term is relatively large.

VI. CONCLUSIONS

In this article a distributed local Kalman consensus filtering algorithm is designed for large-scale multi-agent traffic estimation. The DLKCF is applied on the switching mode model to monitor traffic on a road network partitioned into local sections, with overlapping regions between neighbors introduced to allow for information exchange on measurements and estimates. We prove that the error dynamics of the DLKCF is globally asymptotically stable when all sections switch among observable modes of the SMM. For an unobservable section, we show that the estimates are ultimately bounded, thus ensuring physically meaningful estimates. Numerical experiments verify the proved results, and illustrates the effect of the consensus filter on promoting agreement on the estimates among different agents.

REFERENCES

[1] X. Sun, L. Munoz, and R. Horowitz, "Highway traffic state estimation using improved mixture Kalman filters for effective ramp metering control," in *Proceedings of the 42nd IEEE Conference on Decision and Control*, 2003, pp. 6333–6338.

[2] ——, "Mixture Kalman filter based highway congestion mode and vehicle density estimator and its application," in *Proceedings of the American Control Conference*, 2004, pp. 2098 – 2103.

[3] L. Munoz, X. Sun, R. Horowitz, and L. Alvarez, "Piecewise-linearized cell transmission model and parameter calibration methodology," *Transportation Research Record*, no. 1965, pp. 183–191, 2006.

[4] C. F. Daganzo, "The cell transmission model: a dynamic representation of highway traffic consistent with the hydrodynamic theory," *Transportation Research Part B: Methodological*, vol. 28, no. 4, pp. 269–287, 1994.

[5] ——, "The cell transmission model, part II: network traffic," *Transportation Research Part B: Methodological*, vol. 29, no. 2, pp. 79–93, 1995.

[6] J. P. Lebacque, "The Godunov scheme and what it means for first order traffic flow models," in *Proceedings of the 13th International Symposium on Transportation and Traffic Theory*, 1996, pp. 647–677.

[7] I. Morarescu and C. Canudas de Wit, "Highway traffic model-based density estimation," in *Proceedings of the American Control Conference*, vol. 3, 2011, pp. 2012–2017.

[8] C. Canudas de Wit, L. R. Leon Ojeda, and A. Kibangou, "Graph constrained-CTM observer design for the Grenoble south ring," *13th IFAC Symposium on Control in Transportation Systems*, 2012.

[9] J. Thai and A. Bayen, "State estimation for polyhedral hybrid systems and applications to the Godunov scheme," in *Proceedings of the 16th International Conference on Hybrid Systems: Computation and Control*, 2013, pp. 143–152.

[10] F. Morbidi, L. L. Ojeda, C. Canudas de Wit, and I. Bellicot, "A new robust approach for highway traffic density estimation," in *Proceedings of the 13th European Control Conference*, 2014, pp. 1–6.

[11] S. Jabari and H. Liu, "A stochastic model of traffic flow: Gaussian approximation and estimation," *Transportation Research Part B: Methodological*, vol. 47, pp. 15–41, 2013.

[12] L. Mihaylova, A. Hegyi, A. Gning, and R. Boel, "Parallelized particle and Gaussian sum particle filters for large-scale freeway traffic systems," *IEEE Transactions on Intelligent Transportation Systems*, vol. 13, no. 1, pp. 36 – 48, 2012.

[13] Y. Wang and M. Papageorgiou, "Real-time freeway traffic state estimation based on extended Kalman filter: a general approach," *Transportation Research Part B: Methodological*, vol. 39, no. 2, pp. 141–167, 2005.

[14] L. Mihaylova, R. Boel, and A. Hegyi, "Freeway traffic estimation within recursive Bayesian framework," *Automatica*, vol. 43, no. 2, pp. 290–300, 2007.

[15] D. B. Work, S. Blandin, O.-P. Tossavainen, B. Piccoli, and A. Bayen, "A traffic model for velocity data assimilation," *Applied Mathematics Research eXpress*, vol. 2010, no. 1, pp. 1–35, 2010.

[16] H. Chen and H. A. Rakha, "Prediction of dynamic freeway travel times based on vehicle trajectory construction," in *Proceedings of the 15th IEEE Conference on Intelligent Transportation Systems*, 2012, pp. 576–581.

[17] Y. Yuan, J. van Lint, R. Wilson, F. van Wageningen-Kessels, and S. Hoogendoorn, "Real-time Lagrangian traffic state estimator for freeways," *IEEE Transactions on Intelligent Transportation Systems*, vol. 13, no. 1, pp. 59–70, 2012.

[18] S. Blandin, A. Couque, A. Bayen, and D. B. Work, "On sequential data assimilation for scalar macroscopic traffic flow models," *Physica D: Nonlinear Phenomena*, vol. 241, no. 17, pp. 1421–1440, 2012.

[19] N. Lynch, *Distributed algorithms*. Morgan Kaufmann Publishers, 1997.

[20] A. Fax and R. M. Murray, "Information flow and cooperative control of vehicle formations," *IEEE Transactions on Automatic Control*, vol. 49, no. 9, pp. 1465–1476, 2004.

[21] N. Santoro, *Design and analysis of distributed algorithms*. Wiley-Interscience, 2007.

[22] M. Mesbahi and M. Egerstedt, *Graph theoretic methods in multiagent networks*. Princeton University Press, 2010.

[23] J. L. Speyer, "Computation and transmission requirements for a decentralized linear-quadratic-Gaussiaon control problem," *IEEE Transactions on Automatic Control*, vol. 24, no. 2, pp. 266–269, 1979.

[24] B. S. Y. Rao, H. F. Durrant-Whyte, and J. A. Scheen, "A fully dencentralized multi-sensor system for tracking and surveillance," *International Journal of Robotics Research*, vol. 12, no. 1, pp. 20–44, 1993.

[25] R. Olfati-Saber, "Distributed Kalman filter with embedded consensus filters," in *Proceedings of the 44th IEEE Conference on Decision and Control, and European Control Conference*, 2005, pp. 8179–8184.

[26] U. A. Khan and J. M. F. Moura, "Distributing the Kalman filter for large-scale systems," *IEEE Transactions on Signal Processing*, vol. 56, no. 10, pp. 4919–4935, 2008.

[27] R. Olfati-Saber, "Distributed Kalman filtering for sensor networks," in *Proceedings of the 46th IEEE Conference on Decision and Control*, 2007, pp. 5492–5498.

[28] ——, "Kalman-consensus filter: optimality, stability, and performance," in *Proceedings of the 48th IEEE Conference on Decision and Control*, 2009, pp. 7036–7042.

[29] P. I. Richards, "Shock waves on the highway," *Operations Research*, vol. 4, no. 1, pp. 42–51, 1956.

[30] M. Lighthill and G. Whitham, "On kinematic waves. II. A theory of traffic flow on long crowded roads," *Proceedings of the Royal Society of London. Series A, Mathematical and Physical Sciences*, vol. 229, no. 1178, pp. 317–345, 1955.

[31] S. Godunov, "A difference method for the numerical calculation of discontinuous solutions of hydrodynamic equations," *Mathematics Sbornik*, vol. 47, no. 3, pp. 271–306, 1959.

[32] G. Boker and J. Lunze, "Stability and performance of switching Kalman filters," *International Journal of Control*, vol. 75, no. 16-17, pp. 1269–1281, 2002.

[33] C. Godsil and G. Royle, *Algebraic graph theory*. Springer, 2001.

[34] R. Olfati-Saber, A. Fax, and R. Murry, "Consensus and cooperation in networked multi-agent systems," *Proceedings of the IEEE*, vol. 95, no. 1, pp. 215–233, 2007.

[35] P. Burridge and A. Hall, "Convergence of the Kalman filter gain for a class of non-detectable signal extraction problems," *IEEE Transactions on Automatic Control*, vol. 32, no. 11, pp. 1036–1039, 1987.

[36] H. Khalil, *Nonlinear systems*, 3rd ed. Prentice Hall, 2002.

[37] R. LeVeque, *Finite volume methods for hyperbolic problems*. Cambridge University Press, 2002.